Investigation on cyclability in $Li_xLa_{1/3}NbO_3$ electrode material for rechargeable lithium ion battery

Masanobu Nakayama [a,b], Yoshiharu Uchimoto [a], Masataka Wakihara [a,*]

[a] *Department of Applied Chemistry, Tokyo Institute of Technology, Ookayama, Meguro-ku, Tokyo 152-8552, Japan*
[b] *Japan Society for the Promotion of Science*

Abstract

In this paper, cyclability of perovskite-type electrode material, $Li_xLa_{1/3}NbO_3$ for lithium ion battery has been investigated. In the case of operation voltage at 3.0–1.25 V, good cyclability was observed and ascribed to the small cell volume change during the lithium insertion/removal process. In situ Nb K-edge X-ray absorption spectra suggested that no significant change in volume were caused by internal structural relaxation of NbO_6 octahedron tilting. On the other hand, the capacity gradually decreased with lithium insertion/removal cycle under the operation voltage of 3.0–0.8 V. From the structural study using X-ray diffraction and Nb K-edge extended X-ray absorption fine structure techniques, excess lithium insertion into perovskite structure lead to local distortion around Nb—O bond, and the cell volume increased slightly. These results imply internal relaxation of NbO_6 octahedra play a crucial role in cyclability.
© 2005 Elsevier B.V. All rights reserved.

Keywords: Lithium ion battery; Cyclability; Perouskite; EXAFS

1. Introduction

In recent years, rechargeable lithium-ion batteries (LIB) using transition metal oxide have been studied intensively because of the increasing demand for use in portable electronic devices [1]. One of the immediate requirements for LIB is improvement of battery life, or cyclability. In this viewpoint, it was well known that spinel-type $Li_{4+x}Ti_5O_{12}$ [2–5] shows good cyclability because of quite small cell volume change during lithium insertion. Therefore, designing an electrode material with small volume change is one option to achieve good cycle performance. However, usually it is difficult because reduction of transition-metal (TM) causes the ionic radius of TM increase during the lithium insertion process.

Nadiri et al. reported that A-site deficient perovskite-type $Li_xLa_{1/3}NbO_3$ electrode material showed quite small volume change during lithium insertion reaction ($\sim$0.4% increase in cell volume for lithium insertion at $x \sim 0.8$) [6]. Recently, we suggested that tilting of NbO_6 octahedron suppress the vol-

ume expansion arising from reduction of Nb ion (see Fig. 1) [7]. Therefore good cyclability is expected for this material.

In present paper, we investigated the cyclability of $Li_xLa_{1/3}NbO_3$ with various operation voltage window. In addition, X-ray diffraction (XRD) and in situ Nb K-edge extended absorption fine structure (EXAFS) technique was adopted to reveal the relationship between crystal structure and cycle performance.

2. Experimental

Parent material, $La_{1/3}NbO_3$, was prepared by conventional solid-state reaction. The mixture of stoichiometric amounts of La_2O_3 and Nb_2O_5 was heated at 1000 °C for 2 h and then at 1300 °C for 24 h in air with intermittent grindings. Phase identification was performed by powder X-ray diffraction (XRD) technique using Rigaku RINT2500V diffractometer with Cu Kα radiation, and single-phase perovskite phase was confirmed.

Electrochemical discharge/charge tests were carried out by galvanostatic method, using coin-type cell at 25 °C. The
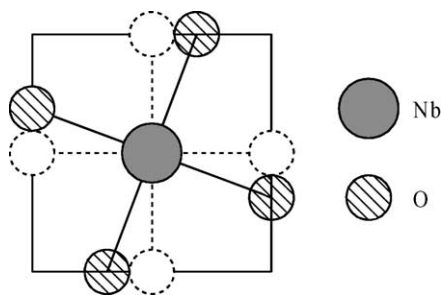

Fig. 1. The schematic image of one of the possible arrangement of ions with NbO_6 octahedral tilting. Figure shows (2 0 0) projection of perovskite structure; solid line indicates the tilting structure and hatched one is the atomic arrangement with cubic symmetry. No matter though Nb ionic radii increase by lithium insertion, tilting of NbO_6 octahedra make it possible to keep the cell volume.

sample powder was mixed with acetylene black (AB) as an electronic conductor and polytetrafluoroethylene as a binder at a weight ratio of 8:1:1. The mixture was coated onto an aluminum sheet, cut into a disk, and then dried under vacuum at 60 °C. This disk and a foil of lithium metal were used as the working and counter electrodes, respectively. The 1 M solution of $LiClO_4$ in anhydrous ethylene carbonate (EC) and diethylene carbonate (DEC) was used as the electrolyte (Tomiyama Pure Chemical Company, Limited).

For structural investigation, XRD and in situ Nb K-edge EXAFS analysis were performed. XRD analysis was carried out using Cu Kβ radiation, since Cu Kα radiation gives split Cu Kα1 and Kα2 diffraction pattern and make it difficult to estimate the lattice parameters with similar a, b, and c parameters ($La_{1/3}NbO_3$ just applies to this case, see Refs. [6,8,9]). Niobium K-edge X-ray absorption spectra for extended X-ray absorption fine structure (EXAFS) technique was measured by transmission mode using synchrotron radiation at BL-10B, Photon Factory, High Energy Accelerator Research Organization, Tsukuba, Japan. For the EXAFS analysis, our own developed in situ electrochemical cell was used. Detailed procedure on XRD and EXAFS structural investigation was mentioned elsewhere [7].

3. Results and discussion

Fig. 2 shows first discharge/charge profiles of $Li|Li_xLa_{1/3}NbO_3$ electrochemical system with two of lithium insertion depths (cut-off voltage = 1.0 V and $x = 0.8$) under the current density of 0.2 mA cm^{-2}. During the first discharge process, the cell potential decreased continuously in the composition range of $0 < x < 0.55$ (solid solution reaction), and a plateau is shown on a boundary up to approximately $x > 0.67$ (two-phase reaction). At the final stage, large polarization was observed at $x \sim 0.67$, indicating that the lithiation into a certain vacant site of perovskite oxides was terminated. Since the composition where the termination occurred agrees with the amount of A-site defect in perovskite $La_{1/3}NbO_3$, lithium ion insertion was made
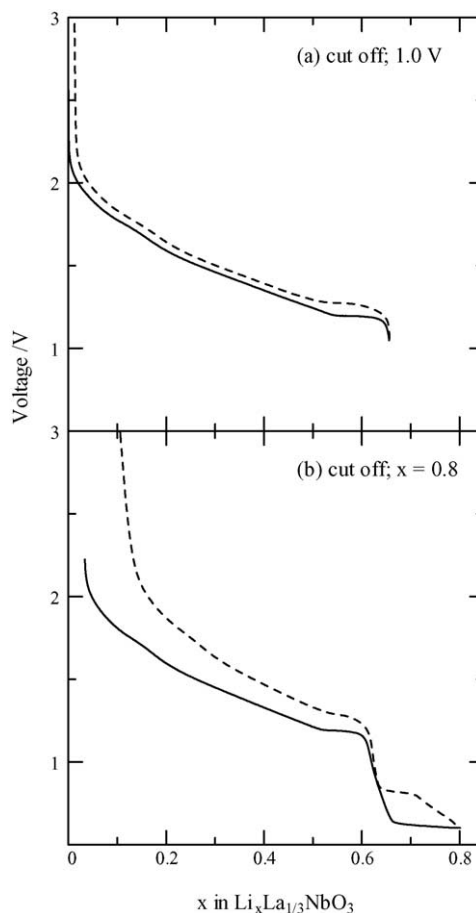

Fig. 2. First discharge/charge diagrams: (a) cut-off voltage = 1.0 V and (b) $x = 0.8$.

into the perovskite A-site. A report concerning the details of lithiation process was already reported elsewhere [10]. In addition, the discharge plateau around 0.6 V (Fig. 1b) would be ascribed to the insertion into AB and/or perovskite 3c-sites (vacant sites at the center of two A-sites) as indicated in previous paper [6,10]. Note that equilibrium potential of the lithium insertion into perovskite 3c vacancy are more than 0.8 V at least [6,10], while large polarization would make the insertion voltage decrease in this experiment. In charge process, good reversibility was observed for the sample lithium inserted into A-site vacancy ($x < \sim 2/3$), while the sample lithium inserted into 3c-site vacancy ($x > \sim 2/3$) shows poor reversibility. In the latter case, the irreversible capacity were observed at not only the plateau around 0.6 V, but also the compositional range, $0 < x < \sim 2/3$ (Li insertion/removal at A site defect in perovskite structure). Therefore, the irreversibility of deep lithium insertion up to 0.6 V might not be caused by the lithium insertion into AB, but by the insertion into perovskite structure (in the later part of this paper, we show clear structural modification of perovskite at ~ 0.6 V region). Cycle performances of the cells $Li|Li_xLa_{1/3}NbO_3$ for cut-off voltage of 3.0–1.0 and 3.0–0.8 V were shown in Fig. 3. In the case of former condition, lithium inserted and removed at A-site vacancy
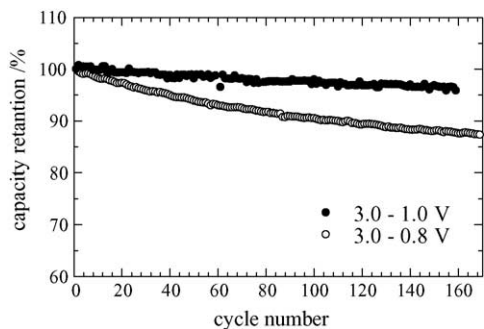
Fig. 3. Rate of capacity retention for perovskite-type electrode, $La_{1/3}NbO_3$, as a function of cycle number. Rate of capacity retention was defined as (capacity in charge process)/(first charge capacity) $\times$ 100 (%).

as mentioned above, and quite good cycle performance was indicated. On the other hand, the capacity decreased gradually with cycle number for the latter cut-off condition. Although no significant amount of excess lithium ion inserted into 3c-site up to $\sim$0.8 V discharge as seen in the Fig. 1b, the cycle performance of $Li_xLa_{1/3}NbO_3$ electrode strongly depended on the operation condition of cut-off voltage. Therefore, quite small amount of excess lithium in perovskite structure plays crucial role for the cycle performance.

To investigate the relationship between cycle performance and structural change, refinement of lattice parameters was performed using XRD measurement (details in Ref. [11]). Fig. 4 showed the changes in cell volume of the samples during first discharge process. The samples for $x = 1.0$ were obtained after potentiostatic discharge upto 0.6 V to complete full lithium insertion into perovskite material (current density was also controlled to keep <0.2 mA cm^{-2} condition). As seen in the figure, the cell volume tended to decrease continuously during the insertion into A-site vacancy ($x < 2/3$), while 3c-site vacancy insertion made the cell expanded ($x > 2/3$). However, the absolute cell volume change is quite small, less than $\pm$0.7%. Note that the cell volume decrease is surprising considering the reduction of Nb^{5+} makes ionic radii increase. This behavior can be understood by the concept of tilting of NbO_6 octahedra as mentioned before (Fig. 1, see Ref. [7]). On the other hand, it was speculated that the mechanism of

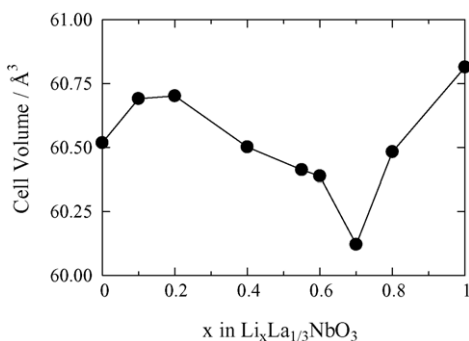Fig. 4. Variation of cell volume (per $Li_xLa_{1/3}NbO_3$ unit). The $x = 1.0$ sample was obtained by potentiostatic discharge at 0.6 V.
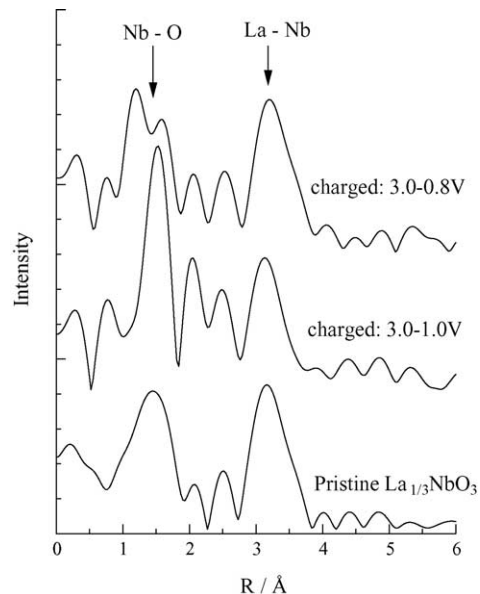

Fig. 5. FT spectra of EXAFS analysis for parent and first-charged samples. First-charged samples were obtained two ways, (1) discharged up to 1.0 V (potentiostatic method) and then charged to 3.0 V and (2) discharged up to 0.8 V and then charged 3.0 V. During the potentiostatic charge/discharge process, the current density was controlled to keep < 0.2 mA cm^{-2}.

tilting did not work well in the case of insertion into 3c-site, as a result the cell volume increased in this region ($x > 2/3$).

Rietveld refinement of XRD measurement for electrochemically reacted samples is usually difficult due to the existence of impurity phase, current collector AB and binder PTFE. To investigate the internal structure, or atomic arrangement in the lattice, we implemented the in situ Nb K-edge EXAFS analysis for the pristine and first-charged samples (cut-off: 3.0–1.0 and 3.0–0.8 V). Fig. 5 shows the Fourier-transformed spectra. From the simulation results using FEFF [12] and REX2000 [13] code, two major peaks were ascribed to the Nb–O and Nb–La interaction, respectively. Two small peaks between Nb–O and Nb–La peaks were assigned as so-called 'ghost peak' arising from Fourier transformation, and quite smaller value in interatomic distance of Nb–O and Nb–La than expected is due to no correction of the phase-shift effect. Details on analysis were described in our previous paper [7]. As seen in the figure, slight increase of interatomic distance was observed between pristine one and cycled one with the cut-off: 3.0–1.0 V, however, main peak feature preserved before and after electrochemical cycling. On the other hand, peak split of Nb–O interaction was observed in the case of 3c-site insertion during first cycle (cut-off: 3.0–0.8 V). This might imply that an irreversible local distortion around Nb–O bond occurred during the 3c-site insertion process.

Summing up above results, the cyclability of $Li_xLa_{1/3}NbO_3$ strongly depends on the depth of discharge process. Long life cycle performance was observed as long as lithium inserted and removed in the A-site vacancy, because tilting of octahedral prevents large cell volume change, which was indicated in our previous paper

[7]. While decay of capacity retention occurred in case of lithium insertion into 3c-site vacancy, and this behavior would be ascribed to the irreversible structural modification around Nb−O bond.

Acknowledgments

References

[1] M. Wakihara, L. Guohua, H. Ikuta, in: M. Wakihara, O. Yamamoto (Eds.), Lithium Ion Batteries, Kodansha, Tokyo, 1998, Chapter 2.

[2] T. Ohzuku, A. Ueda, N. Yamamoto, Y. Iwakoshi, J. Power Sources 54 (1995) 99.

[3] K. Kanamura, H. Naito, Z. Takehara, Chem. Lett. 1 (1997) 45.

[4] T. Ohzuku, A. Ueda, N. Yamamoto, J. Electrochem. Soc. 142 (1995) 1431.

[5] S. Scharner, W. Weppner, P. Schmid-Beurmann, J. Electrochem. Soc. 146 (1999) 857.

[6] A. Nadiri, G. Le Flem, C. Delmas, J. Solid State Chem. 73 (1998) 338.

[7] M. Nakayama, H. Ikuta, Y. Uchimoto, M. Wakihara, Y. Terada, T. Miyanaga, I. Watanabe, J. Phys. Chem. B 107 (2003) 10715.

[8] P.N. Iyer, A.J. Smith, Acta Crystallogr. 23 (1967) 740.

[9] R.A. Dilanian, A. Yamamoto, F. Izumi, T. Kamiyama, Mol. Cryst. Liq. Cryst. 341 (2000) 225.

[10] M. Nakayama, K. Imaki, H. Ikuta, Y. Uchimoto, M. Wakihara, J. Phys. Chem. B 106 (2002) 6437.

[11] M. Nakayama, Thesis, Tokyo Institute of Technology, 2004.

[12] A.L. Ankudinov, B. Ravel, J.J. Rehr, S.D. Conradson, Phys. Rev. B 58 (1998) 7565.

[13] Rigaku EXAFS Analysis Software, REX2000, Cat. No. 2612S311/312/321/322, Rigaku Co., 2000.